Effect of Delignification on the Physical, Thermal, Chemical, and Structural Properties of Sugar Palm Fibre

R. A. Ilyas,[a] S. M. Sapuan,[a,b,*], M. R. Ishak [c], E. S. Zainudin [b]

Eco-friendly composites can be prepared by substituting man-made synthetic fibres with various types of cellulosic fibres. Sugar palm-derived nanocrystalline cellulose is a potential substitute. The most important factor in determining a good nanofiller reinforcement agent that can be used in composites is the character of the nanofiller itself, which is affected during a preliminary treatment. Thus, to gain better nanofiller properties, the delignification ($NaClO_2$ and CH_3COOH) and mercerization (NaOH) treatments must be optimized. The main objective of this study was to identify the effects of the delignification and mercerization treatments on sugar palm fibre (SPF). In addition, the characteristics of the SPF for the preparation of the hydrolysis treatment to produce nanocrystalline cellulose (NCC) for reinforcement in polymer composites were examined. Sugar palm cellulose (SPC) was extracted from the SPF, and its structural composition, thermal stability, functional groups, and degree of crystallinity were determined *via* field emission scanning electron microscopy (FESEM), thermogravimetric analysis (TGA), Fourier transform infrared (FTIR) spectroscopy, and X-ray diffraction (XRD), respectively. The density, moisture content, chemical composition, and structure of the SPC were also analysed.

Keywords: Sugar palm fibre; Delignification; Mercerization; Sugar palm cellulose; Sugar palm acid-treated fibres

*Contact information: a: Laboratory of Biocomposite Technology, Institute of Tropical Forestry and Forest Products (INTROP), Universiti Putra Malaysia, 43400 UPM Serdang, Selangor, Malaysia; b: Department of Mechanical and Manufacturing Engineering, Universiti Putra Malaysia, 43400 UPM Serdang, Selangor, Malaysia; c: Department of Aerospace Engineering, Universiti Putra Malaysia, 43400 UPM Serdang, Selangor, Malaysia; *Corresponding author: sapuan@upm.edu.my*

INTRODUCTION

Environmental concerns over global warming have encouraged researchers to discover new eco-friendly biocomposites with the development of recent technologies (Reddy and Yang 2015; Jumaidin *et al*. 2017c,d). The huge advantages of biocomposites, such as low cost, safety, biodegradability, abundance, light weight, several other intrinsic properties, and preferable properties compared with synthetic fibres, have caused researchers to focus on natural biocomposites (Rajkumar *et al*. 2016; Jumaidin *et al*. 2017a).

However, several problems have been observed when using natural fibres as reinforcement in polymer composites because of their incompatibility. Thus, it is necessary to either modify the surface of the natural fibres or extract their highly crystalline and rigid nanoparticles. The properties of nanocrystalline cellulose (NCC) are dependent upon the type and intensity of the treatment, as well as the preliminary method used to extract the cellulose. One method that was used by several researchers was a delignification and mercerization treatment (Tawakkal *et al*. 2012; Tee *et al*. 2013; Sanyang *et al*. 2016a; R.A. Ilyas *et al*. 2016). Delignification (using sodium chlorite, $NaClO_2$) and mercerization

(using sodium hydroxide, NaOH) treatments can be used to remove the amorphous structure in fibres, such as lignin and hemicellulose, respectively, which also splits the fibres into smaller fibrils known as cellulose microfibrils. Delignification is the process of removing lignin from natural fibre by natural enzymatic or industrial chemical processes. This process penetrates and oxidizes all of the lignin (Keshk *et al.* 2006). Mercerization, also called alkali treatment, is the process of subjecting the natural fibre to the action of fairly concentrated strong base solution (aqueous NaOH or KOH solution), which depend on the type and concentration of solution, temperature and time of treatment, as well as tension of material, to produce great swelling with resultant changes in the fine structure, morphology, dimensions, and mechanical properties; ASTM:D1695-07 (Majeed *et al*. 2013). It has been reported that mercerization has four effects on the fiber: (1) it increases the number of possible reaction sites by exposing the surface of cellulose fibre (2) it increases surface roughness, resultant in better mechanical reinforcement; (3) it improves the mechanical behavior, *i.e.* strength and stiffness, and increases the percentage crystallinity index of alkali treated fibres; and (4) decreases in the spiral angle, *i.e.* closer to fibre axis, and increase in molecular orientation (Akil *et al.* 2011). The removal of the amorphous structure *via* a combination of both treatments greatly increases the crystallinity and purity of the cellulose obtained. There is a correlation between the degree of crystallinity and stiffness of the cellulose, where an increase in the crystallinity increases the stiffness of the fibres. A higher crystallinity in the chemically treated fibres is related to a higher tensile strength. Therefore, the mechanical properties of the nanocomposite material can be improved by using these treated fibres as nanofiller (Rong *et al*. 2001; Bhatnagar and Sain 2005).

Sugar palm trees have been utilized for hundreds of years for manufacturing, and a variety of products can be made from its fibre, trunk, fruit, and palm sap (Tomlinson 1962). This tree is very popular in Negeri Sembilan, Malaysia because palm sap is the material used for making traditional sugar blocks. Additionally, this sugar can be processed into crystal brown sugar, which is used as an alternative to commercialized granular sugar made from sugarcane. Its sap also can be used for making bioethanol, pharmaceuticals, beverages, medicine, biofuel, and several other products under certain processing conditions. Its fibre can be used to make traditional brooms as well. Another important part of the sugar palm is its fruit. The fruit can be used for making juices, canned food, pickles, and dessert. Also, its trunk can be processed for making sago (Ishak *et al*. 2012).

However, the crucial part of the sugar palm tree is its fibre, which is locally known as ijuk. The fibre is black in colour and it can be used for paint brushes, brushes, roofing, handcrafts, ropes, septic tank base filters, and fishing tools (Miller 1964). According to Ishak *et al*. (2012), there are several advantages of the sugar palm fibre (SPF); it has a high durability, good resistance to sea water, high tensile strength, low degradation rate, and is not affected much by moisture and heat compared with coir fibres. It has unique features and does not need to undergo secondary processing, such as mechanical decorticating and water retting, to yield fibre (Ishak *et al*. 2012). This fibre can be readily used because it can easily be found covering the base of palm leaf ribs. Several studies have focused on the properties of raw and treated SPF and its composition to reveal its potential performance and promote its use (Rashid *et al*. 2016; Sanyang *et al*. 2016b).

The main objective of this study is to understand the effects of delignification and mercerization on the physicochemical and thermal properties of SPF. Its characteristics are examined for the preparation of a hydrolysis treatment to produce NCC for the reinforcement of polymer composites. Surface-modified SPF was subjected to physical,

chemical, and thermal stability analyses using X-ray diffraction (XRD), Fourier transform infrared (FTIR) spectroscopy, chemical composition analysis, and thermogravimetric analysis (TGA). Field emission scanning electron microscopy (FESEM) was used to examine the surface of the fibre after treatment.

EXPERIMENTAL

Materials

The SPF used in this study was collected from Jempol, Negeri Sembilan, Malaysia. The chemical reagents used were sodium chlorite ($NaClO_2$), acetic acid (CH_3COOH), and sodium hydroxide (NaOH), which were supplied by Sigma Aldrich (Selangor, Malaysia).

Methods

The cellulose fibres were extracted from the SPF using two main processes, which were delignification and mercerization (Tawakkal *et al*. 2012; Tee *et al*. 2013; Sanyang *et al*. 2016a). The initial process was performed in accordance with ASTM D1104-56 (1978) to prepare holocellulose with a chlorination or bleaching process, which is primarily designed to remove lignin from SPF. Twenty grams of SPF was rinsed with tap water to remove foreign particles and dust. The clean SPF was then soaked in a 1000-mL beaker containing 650 mL of hot distilled water, which was then transferred to a water bath and the temperature was set to 70 °C. Next, 4 mL of acetic acid and 8 g of sodium chlorite were added to the beaker every hour. There were three different treatment times, 5 h, 6 h, and 7 h, and the treated fibres were labelled as sugar palm bleached fibre 05 (SPBF05), sugar palm bleached fibre 06 (SPBF06), and sugar palm bleached fibre 07 (SPBF07), respectively. The cellulose obtained was referred to as holocellulose, and was filtered, washed, and rinsed with distilled water.

The holocellulose was further treated to produce α-cellulose according to ASTM D1103-60 (1977). The holocellulose was soaked in 500 mL of 5% w/v NaOH solution for 2 h at 23 °C ± 2 °C. The α-cellulose that was produced was filtered and immersed in 500 mL of distilled water containing approximately 7 mL of acetic acid to neutralize the alkaline cellulose. The mixture was stirred for approximately 30 s before it was allowed to settle for 5 min. It was then rinsed with water until the cellulose residue was no longer acidic, as indicated by a pH meter. The sugar palm cellulose (SPC) obtained from the fibre treated for 5 h, 6 h, and 7 h was denoted as SPC05, SPC06, and SPC07, respectively. Finally, the cellulose was oven-dried at 103 °C overnight.

Field emission scanning electron microscopy (FESEM)

The FESEM micrographs were taken using an FEI NOVA NanoSEM 230 machine (FEI, Brno-Černovice, Czech Republic) with an accelerating voltage of 3 kV to observe the micro- and nanostructure surfaces of the longitudinal cross-section of the dried SPF and treated fibre. All of the samples were coated with gold using an argon plasma metallizer (sputter coater K575X) (Edwards Limited, Crawley, United Kingdom) to avoid charging (Sheltami *et al*. 2012).

Moisture content

Five samples were prepared for the moisture content investigation. All of the samples were heated in an oven for 24 h at 105 °C. The weight of the samples before (M_i,

gram) and after (M_f, gram) heating were measured to determine the moisture content (Jumaidin *et al*. 2017b), which was calculated using Eq. 1:

$$\text{Moisture content (\%)} = \frac{M_i - M_f}{M_i} \times 100 \quad (1)$$

Density

The density was measured using gas intrusion under a helium gas flow with an AccuPyc 1340 pycnometer (Micromeritics Instrument Corporation, Norcross, GA, USA). Five measurements were taken at 27 °C, and the average value was computed (Jumaidin *et al*. 2017b).

Chemical composition

The chemical composition was analysed according to the TAPPI T222 (2006) (acid-insoluble lignin in wood and pulp) and TAPPI T203 (1999) (α-, β-, and γ-cellulose in pulp) standard methods, and the method described by Wise *et al*. (1946) (holocellulose in pulp).

Fourier transform infrared (FTIR) spectroscopy analysis

The FTIR spectroscopy was used to detect possible changes in the functional groups in the SPF at different stages of treatment. The spectra were obtained using an IR spectrometer (Nicolet 6700 AEM, Thermo Nicolet Corporation, Madison WI, USA). The FTIR spectra of the samples were collected in the range of 4000 cm^{-1} to 500 cm^{-1} with a resolution of 4 cm^{-1} with a total of 42 scans for each sample (Jumaidin *et al*. 2017a,c).

X-Ray diffraction (XRD)

A Rigaku D/max 2500 X-ray powder diffractometer (Rigaku, Tokyo, Japan) operated at a generator voltage of 40 kV, a current of 40 mA, and goniometer speed of 0.02 $(2\theta)s^{-1}$ and equipped with CuKα radiation (λ = 0.1541 nm) in the 2θ range of 10° to 40° was used to study the X-ray diffraction patterns of the raw, bleached, and alkali-treated SPF. An empirical method (Segal *et al*. 1959) was used to obtain the crystallinity index of the samples (X_c), as shown by Eq. 2,

$$X_c = \frac{I_{002} - I_{am}}{I_{002}} \times 100 \quad (2)$$

where I_{002} and I_{am} are the peak intensities of the crystalline and amorphous regions, respectively.

Degree of polymerization (DP)

The degree of polymerization (DP) for each treated fibres suspension was measured based on the intrinsic viscosity. Measurements of viscosity for resulting treated fibres suspension was carried on according to TAPPI Standard Method T230 om-08 and ISO 5351-1 as reported by Chauve *et al*. (2013). The treated fibres were diluted in solutions containing distilled water and copper (II) ethylenediamine (CED) solution as dissolving agent with a ratio 0.01:1:1 (treated fibre: distilled water: CED). The solution was shaken until all the fibres were completely dissolved. The viscosity of this solution and the solvent was measured at 25 °C using Ubbelohde viscometer tube (Type 231, PTA Laboratory Equipment, Vorchdorf, Austria). The experiment was performed for all the samples and

repeated three times. The molecular weight of treated fibre was calculated using the Mark-Houwink approach, which was using Eq. 3,

$$[\eta] = KM^{\alpha} \quad (3)$$

where $[\eta]$ the intrinsic viscosity and M is the molecular weight. The values of the constants were taken as K=0.42 and α=1 for the CED solvent (Yasim-Anuar *et al*. 2017).

Thermogravimetric analysis (TGA)

The thermal degradation behaviour of the composites was analysed with TGA according to the weight loss because of the increase in temperature. The TGA was performed on a Q series thermal analysis machine from TA Instruments (Mettler-Toledo AG, Schwerzenbach, Switzerland) to determine the thermal stability of the SPF at different stages of the extraction. The analysis was performed in aluminium pans under a dynamic nitrogen atmosphere from 25 °C to 600 °C at a heating rate of 10 °C/min (Jumaidin *et al*. 2017a,c).

RESULTS AND DISCUSSION

Physical Properties

The bleaching and alkali treatments not only caused changes in the chemical composition of the treated fibres (SPBF and SPC), they also affected the structure of the surface of the fibres. Figure 1 shows the sugar palm tree, untreated raw SPF, SPBF, and SPC. The pigment of the SPF was altered from black to light brown after the bleaching treatment, and became white after the alkali treatment.

Table 1. Physical Properties of the Sugar Palm Fibre, Bleached Fibre, Alkali-treated Fibre, and Other Biomaterials

Sample	Diameter (μm)	Density (g/cm^3)	Moisture Content (wt.%)	Reference
SPF	212.01 ± 2.17	1.50	8.36	Current study
SPBF05	122.95 ± 0.05	1.36	6.13	Current study
SPBF06	104.45 ± 0.02	1.33	6.27	Current study
SPBF07	94.49 ± 0.03	1.30	6.25	Current study
SPC05	11.84 ± 2.48	1.36	4.19	Current study
SPC06	10.68 ± 2.27	1.32	4.31	Current study
SPC07	8.81 ± 1.65	1.28	3.83	Current study
Kenaf cellulose	17.38	-	-	Tee *et al*. (2013)
Cellulose microfibres	10.04	-	-	Sonia and Dasan (2014)
Coir cellulose	3 to 12	-	-	Sonia and Dasan (2014)
Wheat straw cellulose	6 to 7	-	-	Alemdar and Sain (2008)
Soy hull cellulose	2 to 9	-	-	Alemdar and Sain (2008)
Banana cellulose	10	-	-	Deepa *et al*. (2011)

Results expressed as the mean ± the standard deviation

Fig. 1. Photographs of the (a) sugar palm tree; (b) raw SPF; bleached fibre: (c) SPBF05, (d) SPBF06, and (e) SPBF07; and alkali-treated fibre: (f) SPC05, (g) SPC06, and (h) SPC07

The morphology of the SPF, SPBF05, SPBF06, SPBF07, SPC05, SPC06, and SPC07 were analysed using FESEM. As shown in Table 1, the average diameters of the SPF, SPBF05, SPBF06, SPBF07, SPC05, SPC06, and SPC07 were approximately 212.01 ± 2.17, 122.95 ± 0.05, 104.45 ± 0.02, 94.49 ± 0.03, 11.84 ± 2.48, 10.68 ± 2.27, and 8.81 ± 1.65 µm, respectively. The most apparent difference between the SPF, SPBF, and SPC was a reduction in the diameter.

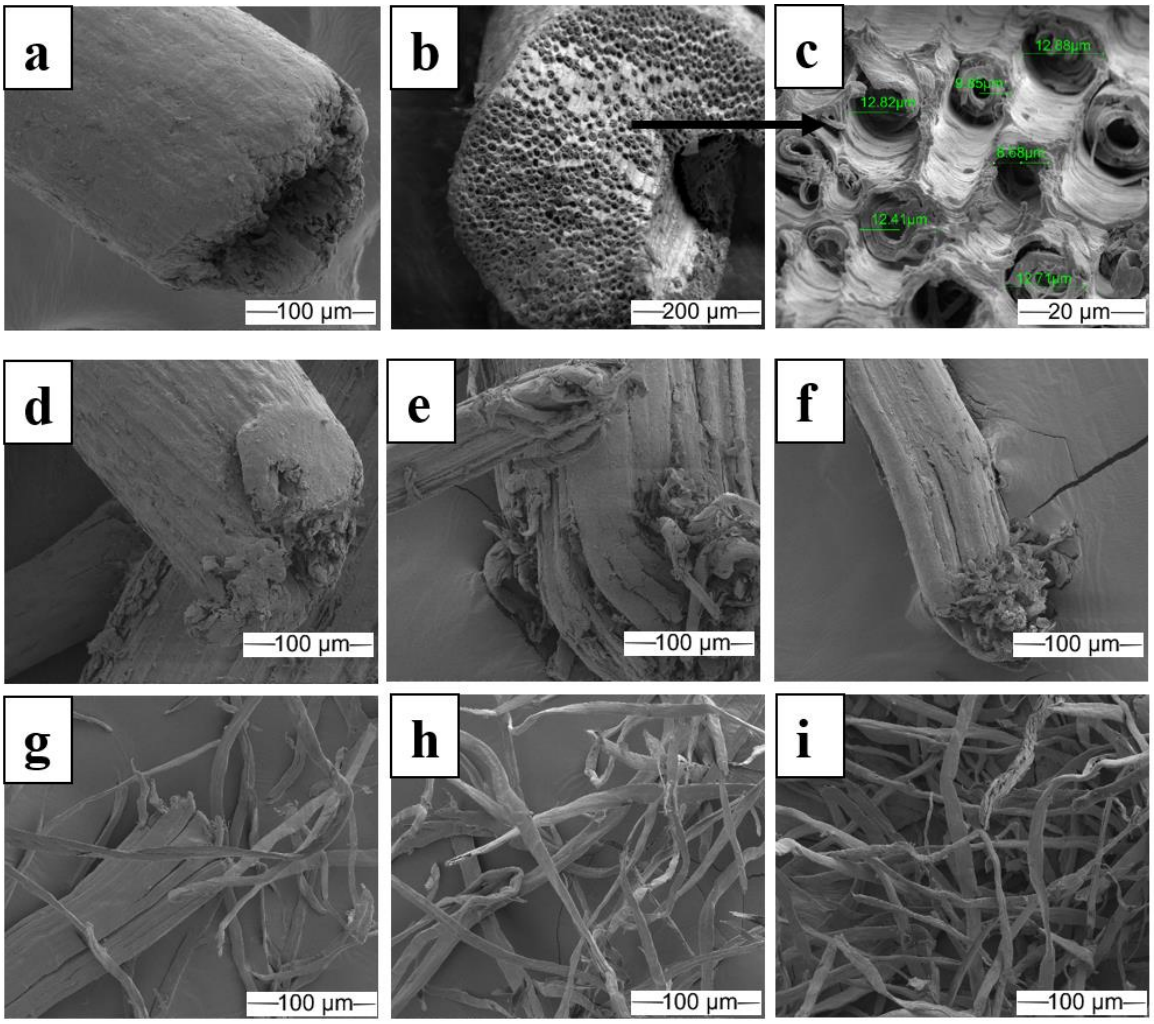

Fig. 2. FESEM micrographs of the raw SPF: (a) longitudinal section, (b) cross section, and (c) primary and secondary cell walls; bleached fibre: (d) SPBF05, (e) SPBF06, and (f) SPBF07; and alkali-treated fibre: (g) SPC05, (h) SPC06, and (i) SPC07

From Table 1, it was clearly seen that the diameter of the SPBF and SPC was almost 2 and 20 times smaller than the diameter of the SPF, respectively. Table 1 showed that there was a slight decrease in the diameter of SPBF05, SPBF06, and SPBF07. This was caused by the increased reaction time of $NaClO_2$ on the fibre, which removed lignin from the SPF. The longer the reaction time of $NaClO_2$, then the smaller the diameter of the fibres. It was reported in previous literature that the treatment method with $NaClO_2$ under acidic conditions has successfully been used to remove lignin from natural fibres (Keshk *et al*. 2006; Liu *et al*. 2012).

The diameter obtained for the SPC was almost similar to the average diameter of kenaf cellulose (13 µm) (Tawakkal *et al*. 2012), coir cellulose (3 µm to 12 µm) (Sonia and Dasan 2014), cellulose microfibres (10.04 µm) (Sonia and Dasan 2014), soy hull cellulose (3 µm to 12 µm) (Alemdar and Sain 2008), and banana cellulose (10 µm) (Deepa *et al*. 2011). Alemdar and Sain (2008) reported a 6 µm to 7 µm diameter for cellulose microfibres, which is less than the diameter of the SPC found in this study. The decreasing trend observed for the diameter of SPBF05, SPBF06, and SPBF07 was ascribed to the removal of lignin and hemicellulose *via* the delignification and mercerization of the raw

SPF, where the SPF bundle was cleaved and cellulose microfibrils were released (Talib *et al*. 2011). These trends were the same as the trends observed for the SPBF because SPC was obtained by continuing the process used to obtain SPBF.

The surface topography of the rod-like SPFs was rough, and hole-like spots that appeared were evenly arranged. Similar spots were also reported on the surface of coir and SPF by Ticoalu *et al*. (2012). According to Ticoalu *et al*. (2012), these observable spots on the surface of the fibres cover the pit on the cell wall, and they are known as tyloses. However, after the fibres went through the process of delignification and mercerization, the surface topography of the derived SPBF and SPC became smooth and groovy, respectively, and parallel lines appeared along the length of the SPBF and SPC (Tee *et al*. 2013; Sanyang *et al*. 2016a). For the surface topography, SPBF had a smooth surface. This was due to the removal of impurities, such as pectin, lignin, and waxy constituents, from the surface of the cell walls after the acid treatment (Tee *et al*. 2013). However, the cellulose microfibrils in the fibres were still arranged in a bundle form. The SPF is generally composed of coarse bundles of single fibres held together by lignin and pectin. Therefore, when sodium chlorite and acetic acid are used directly, the sodium chlorite penetrates and oxidizes all of the lignin (Keshk *et al*. 2006). The groovy surface of the SPC was due to the removal of lignin and hemicellulose (Liu *et al*. 2004; Sgriccia *et al*. 2008; Talib *et al*. 2011; Sanyang *et al*. 2016a). These observations were supported by several authors who studied the surface appearance of natural fibre-derived cellulose (Sgriccia *et al*. 2008; Tawakkal *et al*. 2012; Tee *et al*. 2013; Sanyang *et al*. 2016a).

The moisture content is an important feature that should be taken into account when determining if a natural material is an appropriate filler for polymer composites. It has been reported that the stability, dimensions, porosity formation, and tensile strength of a biocomposite can decline if the biocomposite has a high moisture content (Razali *et al*. 2015; Jumaidin *et al*. 2017b). Hence, a lower moisture content is required. The moisture contents of the SPF, SPBF, and SPC in this study (Table 1) were low (8.36 wt.%, 6.13 wt.% to 6.25 wt.%, and 3.83 wt.% to 4.19 wt.%, respectively) compared with other natural fibres (sisal, jute, flax, banana, nettle, hemp, and ramie fibres), which have a moisture content of approximately 8 wt.% to 22 wt.% (Li *et al*. 2000; Akil *et al*. 2011). This might have been due to the initial heating of the fibres that eliminated some of the moisture. The raw SPF had a slightly higher moisture content than the treated fibre (SPBF and SPC), which indicated that the loss of unstable compounds during the delignification and mercerization treatments also reduced the moisture content. Therefore, the low moisture content possessed by SPBF and SPC make them good prospective fillers in polymer composites.

Additionally, one of the most vital factors that should be taken into account before considering a new material as a filler in polymer composites is their weight, as this property may affect the attainment of the end product. The density of the material is directly associated with the weight. Table 1 displays the average density of the SPF, SPBF05, SPBF06, SPBF07, SPC05, SPC06, and SPC07, which were approximately 1.50, 1.36, 1.33, 1.30, 1.36, 1.32, and 1.28 g/cm^3, respectively. These values were similar to other fibres, such as abaca, flax, cotton, sisal, and ramie, that have a density of 1.5 g/cm^3 (Akil *et al*. 2011; Faruk *et al*. 2012). However, the density of the SPF, SPBF, and SPC were lower compared with man-made fibres, such as E-glass (2.55 g/cm^3) and carbon (1.78 g/cm^3), but slightly higher than other natural fibres, such as oil palm empty fruit bunch (0.7 g/cm^3), coir (1.15 g/cm^3), and bagasse (1.25 g/cm^3) (Akil *et al*. 2011; Faruk *et al*. 2012). Moreover, it was observed that the treated fibre (SPBF and SPC) had slightly lower densities than the

raw SPF. In addition, the density value of the bleached fibres (SPBF05, SPBF06, and SPBF07) and alkali-treated fibres (SPC05, SPC06, and SPC07) showed a decreasing trend. This decreasing trend in density might have been because of the removal of the main components from the fibres, such as lignin and hemicellulose, as shown in Table 1. The removal of cellulosic components during the bleaching and alkali treatments created voids in the fibre structure, which caused fibre swelling to occur. The constituents of the fibres then became very separated. The increased volume and weight loss caused the density value to decrease (Ray and Sarkar 2001).

Chemical Compositions

The chemical composition is a crucial criterion that influences the thermal, physical, and mechanical properties of natural fibres. Plant fibres are composite constituents constructed by nature. Generally, fibres are composed of a matrix of crystalline cellulose microfibrils reinforced with hemicellulose and amorphous lignin (Cristaldi *et al*. 2010). However, the different amounts of these compounds depend on the growth conditions (sources, climate, soil features, and dietary and aging conditions) and fibre processing/extraction methods (Mukherjee and Radhakrishnan 1972; Cristaldi *et al*. 2010; Ishak *et al*. 2012; Razali *et al*. 2015). Table 2 displays the results of the chemical composition analysis of the raw and treated SPF.

Table 2. Comparison of the Chemical Compositions of the Treated and Untreated Sugar Palm Fibre

Sample	Cellulose (%)	Hemicellulose (%)	Holocellulose (%)	Lignin (%)	Ash (%)
SPF	43.88	7.24	51.12	33.24	1.01
SPBF05	54.08	23.05	77.13	2.78	2.06
SPBF06	56	19.92	75.92	1.2	2.14
SPBF07	56.67	19.8	76.47	0.27	2.16
SPC05	80.96	3.26	84.22	1.03	0.94
SPC06	80.47	4.08	84.55	0.41	1.05
SPC07	82.33	3.97	86.3	0.06	0.72

From Table 2, it was seen that SPBF07 and SPC07 had the highest cellulose contents in the SPBF and SPC groups, and were 56.67% and 82.33%, respectively. The cellulose contents for SPC06, SPC05, SPBF06, SPBF05, and SPF were 80.47%, 80.96%, 56%, 54.08%, and 43.88%, respectively. In addition, higher amounts of cellulose were observed in the treated fibre (SPBF and SPC) compared with the raw SPF. This finding may have been due to the removal of some extractive components from the raw SPF during the delignification and mercerization treatments, which separated a higher proportion of the insoluble compounds in the treated fibre (Tan and Lee 2014). Thus, SPBF07 and SPC07 are the preferred fibres to be used for the preparation of NCCs *via* hydrolysis.

FTIR Spectroscopy Analysis

Figure 3 shows the fingerprints of the functional groups in the raw and treated SPF, and Table 3 displays a summary of the assigned FTIR bands. The band located at 1719 cm^{-1} in the raw SPF spectrum is attributed to the C=O stretching of the acetyl and uronic ester groups of the hemicellulose or the ester linkage of the carboxylic groups of ferulic and p-coumaric acids of lignin and/or xylan in the hemicellulose (Sun *et al*. 2005; Alemdar and Sain 2008; Fabiyi and Ogunleye 2015). This band was still present in the FTIR spectra

of the fibres after the bleaching treatment, but it was no longer present after the alkali treatment. The disappearance of this band could have been caused by the removal of hemicellulose and lignin from the SPF during chemical extraction (Alemdar and Sain 2008; Jonoobi *et al*. 2009; Sheltami *et al*. 2012). This was supported by the results obtained from the chemical composition analysis of the fibres (*Chemical Compositions* and Table 2), in which it was indicated that lignin was almost completely removed after the bleaching treatment. However, hemicellulose was still present after the bleaching and alkali treatments. For this reason, the disappearance of the C=O stretching band from the spectra could have been caused by the cleavage of the ester-linked substances of the hemicellulose *via* the alkali treatment. The ether bonds between lignin and hemicellulose were not affected by this treatment (Xiao *et al*. 2001; Sheltami *et al*. 2012).

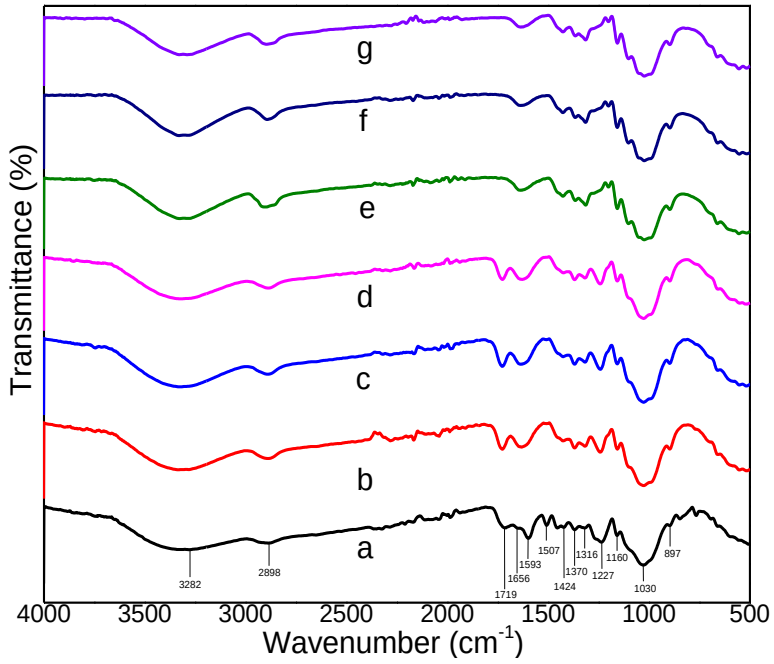

Fig. 3. FTIR spectra of the (a) raw SPF; bleached fibre: (b) SPBF05, (c) SPBF06, and (d) SPBF07; and alkali-treated fibre: (e) SPC05, (f) SPC06, and (g) SPC07

The peaks in the 1520 cm^{-1} to 1510 cm^{-1} region were determined to be aromatic skeletal vibrations of the lignin and lignocellulosic functional groups. The bands observed at 1227 cm^{-1}, 1507 cm^{-1}, and 1593 cm^{-1} corresponded to lignin (Faix *et al*. 1992; Arya *et al*. 2012). These peaks disappeared after the bleaching treatment, which suggested that this treatment effectively removed lignin from the fibres. This conclusion was supported by the chemical composition analysis of the fibres, shown in Table 2. Additionally, the peaks at 1600 cm^{-1} to 1475 cm^{-1} were determined to be the structural polymer stretching of the aromatic groups present in the form of lignin (Himmelsbach *et al*. 2002; Sahari *et al*. 2012).

Based on Fig. 4 and Table 3, the absorbance peaks in the region from 1650 cm^{-1} to 1630 cm^{-1} and at approximately 2900 cm^{-1} reflected the stretching of O–H and C–H groups, respectively. The peaks in the 3700 cm^{-1} to 3100 cm^{-1} region were assigned to adsorbed water. The peaks at 897, 1030, 1160, 1316, 1370, and 1424 cm^{-1} were attributed to the C–H rocking vibrations, C–O stretching, C-O-C asymmetric valence vibration, C-H_2 rocking vibration, C-H_2 deformation vibration, and cellulose in the carbohydrates,

respectively (Alemdar and Sain 2008; Sheltami *et al*. 2012). These different bands were seen in all of the spectra, regardless of the treatment of the fibres. The intense peak at 1656 cm^{-1} signified C=C stretching of unsaturated acids or sterols corresponding to tannin (Sun and Tomkinson 2002).

Table 3. Summary of the IR Bands Observed for the Bleached and Alkali-treated Sugar Palm Fibre

Peak Assignment	Wavenumber (cm^{-1})	Structural Polymer	Reference
Cellulose	897	C–H rocking vibrations	Fengel and Ludwig (1991); Fan *et al*. (2012)
Cellulose	1160	C-O-C asymmetric valence vibration	Faix *et al*. (1992)
Cellulose	1316	$C-H_2$ rocking vibration	Fan *et al*. (2012)
Cellulose	1370	$C-H_2$ deformation vibration	Fan *et al*. (2012)
Cellulose	1424	-	Fan *et al*. (2012)
Cellulose and hemicellulose	1030	C-O stretching of primary alcohol	Faix *et al*. (1992)
Xylan in hemicellulose	1719	C=O stretching of the acetyl	Sheltami *et al*. (2012)
Lignin and lignocellulose	1520 to1510	aromatic skeletal vibration	Faix *et al*. (1992); Ouatmane *et al*. (2000)
Lignin	1227	C-C plus C-O plus C=O stretch; G condensed > G etherified	Faix *et al*. (1992)
Lignin	1507	aromatic skeletal vibration (C=C), guaiacyl > syringyl	Faix *et al*. (1992)
Lignin	1593	aromatic skeletal vibration plus (C=O), stretching; S > G; G condensed > G etherified	Faix *et al*. (1992)
Tannin	1656	C=C cis stretching of unsaturated acids or sterols	Sun and Tomkinson (2002)
-	2897	C–H stretching in methyl and methylene groups	Faix *et al*. (1992)
-	1650 to 1630	O–H	Sahari *et al*. (2012)
-	3500 to 3200	O–H	Sahari *et al*. (2012)

The intense peaks at 3500 cm^{-1} to 3200 cm^{-1} indicated the presence of O-H groups in the untreated and treated fibres because of the presence of hydroxyl groups in the cellulose, hemicellulose, and lignin. The peaks at 1800 cm^{-1} to 1600 cm^{-1} signified carbonyl groups (C=O) in the lignin and hemicellulose (Kazayawoko *et al*. 1997). The high peaks at 1300 cm^{-1} to 1000 cm^{-1} existed in all of the fibre types, and signified C-H stretching and C-O groups (Faix *et al*. 1992).

XRD Measurements

The crystallinity of individual fibres can influence the thermal and mechanical properties of a composite. Therefore, an XRD study was conducted to investigate the crystallinity of the raw and treated SPF. The XRD graph (Fig. 4) showed that all of the diffractograms displayed sharp peaks at 2θ values of approximately 16° and 22.8°, which were assumed to signify the typical cellulose I form. In contrast, the amorphous region was characterized by low peaks at a 2θ value of approximately 18° (Segal *et al*. 1959). This showed that the crystalline cellulose structure was not altered by the chemical treatment.

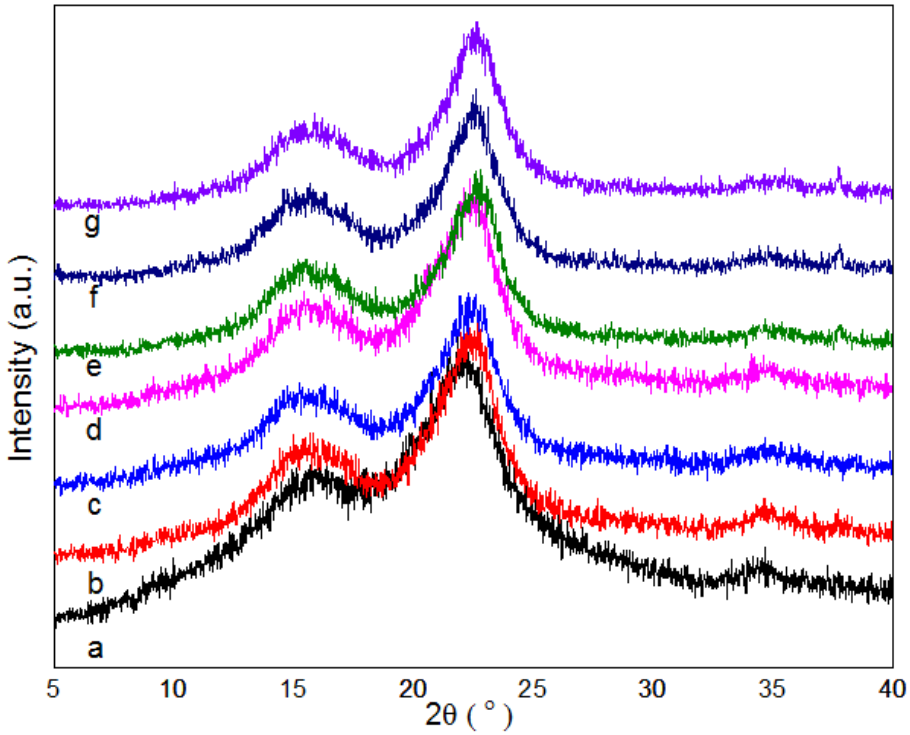

Fig. 4. X-ray diffraction patterns of the (a) raw SPF; bleached fibre: (b) SPBF05, (c) SPBF06, and (d) SPBF07; and alkali-treated fibre: (e) SPC05, (f) SPC06, and (g) SPC07

Table 4. Properties of Cellulose from various Sources

Materials	Main characteristic					Reference
	DP	M_W (g/mol)	2θ (am) (°)	2θ (002) (°)	X_c (%)	
SPF	-	-	17.3	21.8	55.8	Current study
SPBF05	3417.9	554,215	18.0	22.7	64.9	Current study
SPBF06	3164.5	513,137	18.3	22.3	64.8	Current study
SPBF07	2963.3	480,513	18.4	22.3	65.9	Current study
SPC05	1165.7	189,024	18.3	22.8	73.4	Current study
SPC06	1047.9	169,920	18.3	22.6	74.2	Current study
SPC07	946.4	153,458	19.2	22.7	76.0	Current study
Flax	2801	337,440	-	-	67.0	Wang *et al.* (2010)
Bamboo	891	144,478	-	-	53.0	Wang *et al*. (2010)
Oil Palm	967	157,000	-	-	51-55	Yasim *et al*. (2017)

The crystallinity index of each untreated and treated sample was also calculated and listed in Table 4. A noticeable increase in the crystallinity from 55.8% for the raw SPF to 76.0% for the chemically treated cellulose fibres was observed. The crystallinity indices of the raw SPF, SPBF05, SPBF06, SPBF07, SPC05, SPC06, and SPC07 were 55.8%, 64.9%, 64.8%, 65.9%, 73.4%, 74.2%, and 76.0%, respectively. The increase in the crystallinity of the fibres was due to the removal of amorphous substances, such as lignin and hemicellulose, during the delignification and mercerization treatments. This increase in crystallinity after the chemical treatments was supported by several other studies (Alemdar and Sain 2008; Chen *et al*. 2011). Compared with other treatments, SPBF07 and SPC07 had higher crystallinity indices with 65.9% and 76.0%, respectively. This was because of the prolonged delignification treatment time, which removed most of the lignin content from the fibres. The crystallinity index for SPC07 after the alkali treatment was higher than the values of mengkuang leaf (69.5%) and pineapple leaf (54%) fibres reported by Sheltami *et al*. (2012) and Cherian *et al*. (2010), respectively. Additionally, the diffraction peak at 22.6° became sharper after the chemical treatment. This observation was related to the better crystalline domains.

Degree of Polymerization

Degree of polymerization (DP) is a crucial parameter for evaluating the length and branching of cellulose chains. Besides that, it has been stated by Audrey *et al*. (2007), that DP and molecular weight may affect the properties of cellulose such as spinnability, solubility, and the mechanical properties of cellulose based materials. The degree of polymerization and viscosity-average molecular weight of the treated fibres were determined using an intrinsic viscosity measurement. Table 4 gives the DP value for the various treated fibres prepared in this study. The degree of polymerization of the SPBF05, SPBF06, SPBF07, SPC05, SPC06 and SPC07 were 3417.9, 3164.5, 2963.3, 1165.7, 1047.9 and 946.4, respectively, and the molecular weight were 554,200 g/mol, 513,100 g/mol, 480,500 g/mol, 189,000 g/mol, 169,900 g/mol, and 153,500 g/mol, respectively.

From the same table , it can be seen that the DP obtained for the SPC07 was almost similar to the DP of oil palm cellulose (967) (Yasim *et al.* 2017) and bamboo cellulose (891) (Wang *et al.* 2010). According to Yasmin *et al.* (2017) the molecular weight and degree of polymerization of bio-cellulose based material were ranged from approximately 90,000 to 300,000 g/mol and 400 to 3000, respectively. The sugar palm cellulose (SPC05, SPC06 and SPC07) were in the range of the cellulose DP, thus in good agreement with those reported in the literature.

Besides, it has been reported by Kumar *et al.* (2009), that delignification by the acid-chlorite process has a significant effect on the cellulose chain, in which it causes a huge reduction in the average degree of polymerization of treated fibres. Extensive delignification of SPBF07 process reduced the DP to 2963, and further mercerization process caused the DP to decrease to 946.4. The significant reduction in DP is consistent with the reduced treated fibre lengths observed and previously mentioned. In this study, the DP was reduced by more than 68% after 7 h of delignification and mercerization process. The decreasing trend observed for the DP of SPC05, SPC06, and SPC07 was attributed by the removal of lignin and hemicellulose *via* the delignification and mercerization of the raw SPF, where the SPF bundle and SPBF fibres was cleaved and cellulose microfibrils were released (Talib *et al*. 2011). Moreover, the DP reduction of cellulose was also due to the acid catalysed cleavage during acid-chlorite delignification (Hubbell and Ragauskas 2010).

Thermogravimetric Analysis (TGA)

Generally, the thermoplastic handling temperature increases above 200 °C, so it is important to know the thermal properties of the fibres before they are used in biocomposites to determine their compatibility with the thermoplastic itself. The thermal degradation characteristics of the treated and untreated SPF are shown with the TG and DTG curves in Fig. 5. It was observed that the thermal degradation of the treated and untreated fibres had four stages.

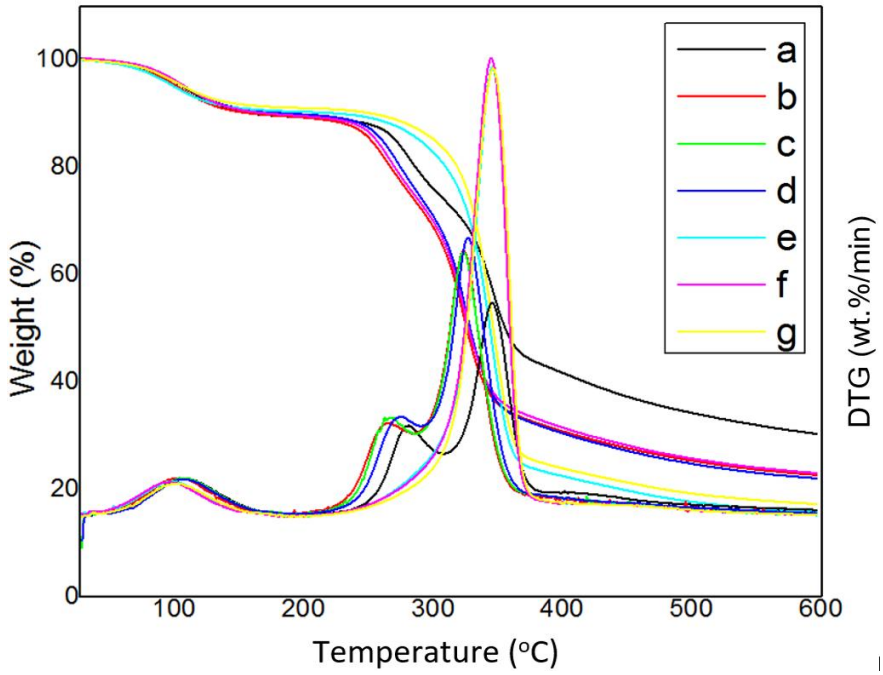

Fig. 5. TG and DTG curves of the (a) raw SPF, bleached fibre, (b) SPBF05, (c) SPBF06, and (d) SPBF07, and alkali-treated fibre: (e) SPC05, (f) SPC06, and (g) SPC07

The first stage was evaporation of the moisture content (45 °C to 123 °C) within the fibre, followed by degradation of the lignocellulosic components of the hemicellulose (220 °C to 315 °C), cellulose (300 °C to 370 °C), lignin (160 °C to 900 °C), and finally the ash (1723 °C). When the fibres were heated, the weight of the fibres gradually decreased because of the loss of water and volatile extractives (Ishak *et al*. 2012). Also, the volatile extractives were less likely to move to the fibre surface. This lack of movement of volatile extractives was because of the movement of water from inside the fibre to the fibre surface, as the water on the fibre surface was vaporized during the heating process. The low-temperature heating process resulted in a low mass loss with only losses of water in the cell lumen and cell wall, and volatile extractives in the fibres. It was observed that the evaporation of moisture from the SPF was completed at 106.78 °C, which was higher compared with the treated fibre (approximately 101 °C), as shown in Table 5. This was because of the high moisture content of the SPF (8.36%), which resulted in a higher weight loss compared with the treated fibres (3.83% to 6.87%), as shown in Table 1. It was observed in Table 5 that the weight loss for the treated fibres ranged from approximately 8.58 wt.% to 10.36 wt.% at approximately 101 °C, while for the SPF, the weight loss was 10.38 wt.% at 106.78 °C. This remarkable weight loss was because of the degradation of the basic lignocellulosic components, starting with hemicellulose, cellulose, and lastly lignin, which generally degrades at 100 °C to 140 °C and higher (Yang *et al*. 2007). It was

observed that the first and secondary thermal degradation onset temperatures of the raw SPF occurred at 210.58 °C and 308.05 °C, respectively. Meanwhile, the DTG curve showed that the onset temperature of the treated fibres shifted to a lower temperature (approximately 195 °C). A slight decrease in the second thermal degradation onset temperature (approximately 284 °C) was also observed. The higher thermal stability of the SPF might have been because of the higher lignin content, which gives rigidity to the plant materials.

Table 5. Onset Temperature (T_{Onset}), Degradation Temperature of the Maximum Weight Loss Rate (T_{Max}), Weight Loss (W_L), and Char Yield for the Sugar Palm Fibre

Sample	Water Evaporation			1st Thermal Degradation			2nd Thermal Degradation			Char Yield
	T_{Onset} (°C)	T_{Max} (°C)	W_L (%)	T_{Onset} (°C)	T_{Max} (°C)	W_L (%)	T_{Onset} (°C)	T_{Max} (°C)	W_L (%)	W (%)
SPF	41.7	106.8	10.4	210.6	281.0	15.1	308.1	345.5	43.8	30.7
SPBF05	41.5	101.4	10.4	196.7	268.2	14.9	284.9	324.3	48.6	26.0
SPBF06	38.2	102.1	10.4	197.5	260.4	15.1	284.4	321.3	51.6	23.0
SPBF07	42.4	103.7	9.9	195.7	271.6	15.2	288.4	324.4	52.4	22.5
SPC05	45.2	99.1	9.2	210.1	346.7	74.4				16.3
SPC06	41.5	98.89	9.2	207.4	346.8	75.4				15.4
SPC07	43.5	101.2	8.6	207.9	345.1	73.7				17.7

Data was obtained from the TG and DTG curves

The second stage was the degradation of hemicellulose. This typically occurs when the temperature is increased to 220 °C, and is completed at 315 °C (Yang *et al*. 2007). However, the results obtained from this study showed that the degradation of hemicellulose occurred from 195.66 °C to 197.54 °C for SPBF05, SPBF06, and SPBF07, and for SPF, hemicellulose began degradation at 210 °C and was completely degraded by approximately 300 °C, as shown in Fig. 5. This stage only occurred for the SPBF and SPF, and not for the SPC because hemicellulose was removed during the alkali treatment. The onset degradation temperature was shifted from 210 °C (SPF) to 195.66 °C (SPBF) after the bleaching treatment. This may have been because of the lower hemicellulose content (7.24%) in the SPF compared with the SPBF (19.8% to 23.05%), as seen in Table 2. Several reasons were determined by Yang *et al*. (2007) for the sequence of lignocellulosic degradation, which starts with hemicellulose. Hemicellulose is comprised of various saccharides, such as mannose, galactose, xylose, and glucose. It appears in an amorphous state and is easy to remove at low temperatures. Also, its lower thermal stability than for cellulose causes hemicellulose to degrade to a greater extent compared with cellulose and lignin (Shafizadeh and Chin 1977).

The third stage was the degradation of cellulose, which started shortly after the hemicellulose had completely degraded. The degradation of cellulose requires higher temperatures, but once the required temperature is attained, degradation happens at a very high rate. It was seen from Table 5 that the cellulose had the highest rate of degradation of the entire degradation process. It was determined by several authors, such as Yang *et al*. (2007) and Ishak *et al*. (2012b), that the highest degradation rate occurred during the degradation of cellulose. In this study, it was observed from the DTG curves of the fibres (Fig. 5) that cellulose degraded from 210 °C to 390 °C, and the highest rate of degradation

occurred at an average temperature of 330 °C. This was supported by Kim *et al*. (2001) and Ishak *et al*. (2012), who reported that the critical temperature for the degradation of cellulose is 320 °C and 330 °C, respectively. A similar temperature was found in this study because the cellulose content in the raw SPF (43.88%) was lower compared to the treated fibres (54.08% to 82.33%) (Table 2) and the weight loss of the cellulose in the raw SPF was found to be lower (43.76 wt.% at 345.45 °C) than for the treated fibre (73.71 wt.% at 345.09 °C). It was also seen in Fig. 5 that there was a noticeable difference in the TG and DTG curves of the treated and untreated fibres. The SPC samples had two more peaks compared with the SPF and SPBF. This was because of the removal of hemicellulose from the fibres during the alkali treatment. It was also seen that among the SPBF, the maximum cellulose degradation (324.44%) occurred for SPBF07. The thermal degradation onset temperature for SPF was similar to that of other natural fibres, such as roselle (220 °C) and kenaf (244 °C).

The fourth phase was the degradation of lignin. Lignin was difficult to degrade compared with hemicellulose and cellulose. The degradation of lignin started as early as 160 °C and continued until 900 °C. The difficulty in degrading lignin may have been because of the toughness of lignin, which mainly functions as support for plants and bonds individual cells together in the middle lamella region. However, lignin degradation occurred at a low weight loss rate (< 0.14 wt.%/°C) from the ambient temperature to 900 °C (Shafizadeh and Chin 1977; Yang *et al*. 2007; Ishak *et al*. 2012). It was observed in Fig. 5 that there were slight differences in the TG and DTG curves of the treated and untreated fibres. The second SPF curve shifted to the right compared with the SPBF curve. This might have been due to the higher lignin content (33.24%) in the SPF fibres compared with the SPBF (0.27% to 2.78%), which prevented the hemicellulose from being easily degraded.

When the lignin had completely degraded, only the leftover material, called char or ash, remained. This char consists of inorganic material, such as silica, which can be degraded at 1723 °C (Ishak *et al*. 2012). Table 5 clearly indicated there was a higher char content for the raw SPF than for the other fibres. Additionally, char also blocked the reactive chemical groups and suppressed the percent weight loss of the fibre. This was the reason why the raw SPF had a higher thermal stability than the treated fibres. These results were consistent with the results obtained from the chemical composition, XRD, and FTIR analyses.

CONCLUSIONS

1. The treated SPF, particularly SPBF07 and SPC07, possessed certain advantages, such as a higher crystallinity, higher purity of cellulose, and better thermal stability, compared with the other fibres.
2. The raw SPF had a slightly higher density and moisture content than the treated fibres. The XRD and FTIR analyses indicated that there were changes to the structure of the fibres during treatment.

ACKNOWLEDGMENTS

The authors would like to thank the Universiti Putra Malaysia for the financial support through the Graduate Research Fellowship (GRF) scholarship. The authors are grateful to Dr. Muhammed Lamin Sanyang for guidance throughout the experiment. The authors also thank the Forest Research Institute Malaysia (FRIM) and Dr. Rushdan Ibrahim for their advice and fruitful discussions.

REFERENCES CITED

Akil, H. M., Omar, M. F., Mazuki, A. A. M., Safiee, S., Ishak, Z. A. M., and Abu Bakar, A. (2011). "Kenaf fiber reinforced composites: A review," *Materials and Design* 32(8–9), 4107-4121. DOI: 10.1016/j.matdes.2011.04.008

Alemdar, A., and Sain, M. (2008). "Isolation and characterization of nanofibers from agricultural residues - Wheat straw and soy hulls," *Bioresource Technology* 99(6), 1664-1671. DOI: 10.1016/j.biortech.2007.04.029

Arya, E. N., Wang, Z. J., and Ward, R. K. (2012). "Image watermarking in higher-order gradient domain," in: *Advances in Wavelet Theory and Their Applications in Engineering, Physics and Technology*, InTech. DOI: 10.5772/35603

ASTM D1104-56 (1978). "Method of test for holocellulose in wood," American Society for Testing and Materials, USA.

ASTM D1103-60 (1977). "Method of test for alpha-cellulose in wood," American Society for Testing and Materials, USA.

ASTM D1695-07(2012), *Standard Terminology of Cellulose and Cellulose Derivatives*, ASTM International, West Conshohocken, PA, 2012

Bhatnagar, A. and Sain, M. (2005). "Processing of cellulose nanofiber-reinforced composites," *Journal of Reinforced Plastics and Composites* 24(12), 1259-1268. DOI: 10.1177/0731684405049864

Chauve, M., Barre, L., Tapin-lingua, S., Perez, S., Decottignies, D., Perez, S., and Ferreira, N. L. (2013). "Evolution and impact of cellulose architecture during enzymatic hydrolysis by fungal cellulases," *Advances in Biosciences and Biotechnology* 4(December), 1095-1109. DOI: 10.4236/abb.2013.412146

Chen, W., Yu, H., Liu, Y., Chen, P., Zhang, M., and Hai, Y. (2011). "Individualization of cellulose nanofibers from wood using high-intensity ultrasonication combined with chemical pretreatments," *Carbohydrate Polymers* 83(4), 1804-1811. DOI: 10.1016/j.carbpol.2010.10.040

Cherian, B. M., Leão, A. L., de Souza, S. F., Thomas, S., Pothan, L. A., and Kottaisamy, M. (2010). "Isolation of nanocellulose from pineapple leaf fibres by steam explosion,"*Carbohydrate Polymers* 81(3), 720-725. DOI: 10.1016/j.carbpol.2010.03.046

Cristaldi, G., Latteri, A., Recca, G., and Cicala, G. (2010). "Composites based on natural fibre fabrics," *Woven Fabric Engineering* 17, 317-342.

Deepa, B., Abraham, E., Cherian, B. M., Bismarck, A., Blaker, J. J., Pothan, L. A., Leao, A. L., de Souza, S. F., and Kottaisamy, M. ((2011). "Structure, morphology and thermal characteristics of banana nano fibers obtained by steam explosion," *Bioresource Technology* 102(2), 1988-1997. DOI: 10.1016/j.biortech.2010.09.030

Fabiyi, J. S., and Ogunleye, B. M. (2015). "Mid-infrared spectroscopy and dynamic

mechanical analysis of heat-treated obeche (*Triplochiton scleroxylon*)wood," *Maderas. Ciencia Y Tecnología* 17(1), 5-16. DOI: 10.4067/S0718-221X2015005000001

Faix, O., Lin, S., and Dence, C. (1992). "Fourier transform infrared spectroscopy," in: *Methods in Lignin Chemistry*, Springer-Verlag, pp. 83-109.

Fan, M., Dai, D., and Huang, B. (2012). *Fourier Transform - Materials Analysis*, S. Salih (ed.), *Fourier Transform - Materials Analysis*. InTech. DOI:10.5772/2659

Faruk, O., Bledzki, A. K., Fink, H.-P., and Sain, M. (2012). "Biocomposites reinforced with natural fibers: 2000–2010," *Progress in Polymer Science* 37(11), 1552-1596. DOI: 10.1016/j.progpolymsci.2012.04.003

Fengel, D., and Ludwig, M. (1991). "Possibilities and limits of FTIR spectroscopy characterization of the cellulose," *Das Papier* 45(2), 45-51.

Himmelsbach, D. S., Khalili, S., and Akin, D. E. (2002). "The use of FT-IR microspectroscopic mapping to study the effects of enzymatic retting of flax (*Linum usitatissimum* L) stems," *Journal of the Science of Food and Agriculture* 82(7), 685-696. DOI: 10.1002/jsfa.1090

Hubbell, C. A., and Ragauskas, A. J. (2010). "Effect of acid-chlorite delignification on cellulose degree of polymerization," *Bioresource Technology* 101(19), 7410-7415. DOI: 10.1016/j.biortech.2010.04.029

Ilyas, R. A., Sapuan, S. M., Sanyang, M. L., and Ishak, M. R. (2016). "Nanocrystalline cellulose reinforced starch-based nanocomposite: A review," in: *5th Postgraduate Seminar on Natural Fiber Composites*, Universiti Putra Malaysia, Serdang, Selangor, 82–87.

Ishak, M. R., Sapuan, S. M., Leman, Z., Rahman, M. Z. A., and Anwar, U. M. K. (2012a). "Characterization of sugar palm (*Arenga pinnata*) fibres," *Journal of Thermal Analysis and Calorimetry* 109(2), 981-989. DOI: 10.1007/s10973-011-1785-1

Ishak, M. R., Sapuan, S. M., Leman, Z., Rahman, M. Z. A., and Anwar, U. M. K. (2012b). "Characterization of sugar palm (*Arenga pinnata*) fibres tensile and thermal properties," *Journal of Thermal Analysis and Calorimetry* 109(2), 981-989. DOI: 10.1007/s10973-011-1785-1

ISO 5351-1 (2004). "Pulps - Determination of limiting viscosity number in cupri ethylenediamine (CED) solution," International Organization for Standardization, Geneva, Switzerland

Jonoobi, M., Harun, J., Shakeri, A., Misra, M., and Oksmand, K. (2009). "Chemical composition, crystallinity, and thermal degradation of bleached and unbleached kenaf bast (*Hibiscus cannabinus*) pulp and nanofibers," *BioResources* 4(2), 626-639. DOI: 10.15376/biores.4.2.626-639

Jumaidin, R., Sapuan, S., Jawaid, M., Ishak, M., and Sahari, J. (2017a). "Effect of agar on flexural, impact, and thermogravimetric properties of thermoplastic sugar palm starch," *Current Organic Synthesis* 14(2), 200-205. DOI: 10.2174/1570179413666160921110732

Jumaidin, R., Sapuan, S. M., Jawaid, M., Ishak, M. R., and Sahari, J. (2017d). "Characteristics of *Eucheuma cottonii* waste from East Malaysia: Physical, thermal, and chemical composition," *European Journal of Phycology* 52(2), 200-207. DOI: 10.1080/09670262.2016.1248498

Jumaidin, R., Sapuan, S. M., Jawaid, M., Ishak, M. R., and Sahari, J. (2017b). "Effect of seaweed on mechanical, thermal, and biodegradation properties of thermoplastic

sugar palm starch/agar composites," *International Journal of Biological Macromolecules* 99, 265-273. DOI: 10.1016/j.ijbiomac.2017.02.092

Jumaidin, R., Sapuan, S. M., Jawaid, M., Ishak, M. R., and Sahari, J. (2017c). "Thermal, mechanical, and physical properties of seaweed/sugar palm fibre reinforced thermoplastic sugar palm starch/agar hybrid composites," *International Journal of Biological Macromolecules* 97, 606-615. DOI: 10.1016/j.ijbiomac.2017.01.079

Kazayawoko, M., Balatinecz, J. J., and Woodhams, R. T. (1997). "Diffuse reflectance Fourier transform infrared spectra of wood fibers treated with maleated polypropylenes," *Journal of Applied Polymer Science* 66(6), 1163-1173. DOI: 10.1002/(SICI)1097-4628(19971107)66:6<1163::AID-APP16>3.0.CO;2-2

Keshk, S., Suwinarti, W., and Sameshima, K. (2006). "Physicochemical characterization of different treatment sequences on kenaf bast fiber," *Carbohydr. Polym.* 65(2), 202-206. DOI: 10.1016/j.carbpol.2006.01.005

Kim, D.-Y., Nishiyama, Y., Wada, M., and Kuga, S. (2001). "High-yield carbonization of cellulose by sulfuric acid impregnation," *Cellulose* 8(1), 29-33. DOI: 10.1023/A:1016621103245

Kumar, R., Mago, G., Balan, V., and Wyman, C. E. (2009). "Physical and chemical characterizations of corn stover and poplar solids resulting from leading pretreatment technologies," *Bioresource Technology* 100(17), 3948-3962. DOI: 10.1016/j.biortech.2009.01.075

Li, Y., Mai, Y. W., and Ye, L. (2000). "Sisal fibre and its composites: A review of recent developments," *Composites Science and Technology* 60(11), 2037-2055. DOI: 10.1016/S0266-3538(00)00101-9

Liu, W., Mohanty, A. K., Drzal, L. T., Askel, P., and Misra, M. (2004). "Effects of alkali treatment on the structure, morphology and thermal properties of native grass fibers as reinforcements for polymer matrix composites," *Journal of Materials Science* 39(c), 1051-1054. DOI: 10.1023/B:JMSC.0000012942.83614.75

Liu, Y., Wang, J., Zheng, Y., and Wang, A. (2012). "Adsorption of methylene blue by kapok fiber treated by sodium chlorite optimized with response surface methodology," *Chemical Engineering Journal* 184, 248-255. DOI: 10.1016/j.cej.2012.01.049

Majeed, K., Jawaid, M., Hassan, A., Abu Bakar, A., Abdul Khalil, H. P. S., Salema, A. A., and Inuwa, I. (2013). "Potential materials for food packaging from nanoclay/natural fibres filled hybrid composites," *Materials & Design* 46, 391-410. DOI: 10.1016/j.matdes.2012.10.044

Miller, R. H. (1964). "The versatile sugar palm," *Principes* 8, 115-146.

Mukherjee, R. R., and Radhakrishnan, T. (1972). "Long vegetable fibres," *Textile Progress* 4(4), 1-75. DOI: 10.1080/00405167208688974

Ouatmane, A., Provenzano, M. R., Hafidi, M., and Senesi, N. (2000). "Compost maturity assessment using calorimetry, spectroscopy and chemical analysis," *Compost Science & Utilization* 8(2), 124-134. DOI: 10.1080/1065657X.2000.10701758

Rajkumar, R., Manikandan, A., and Saravanakumar, S. S. (2016). "Physicochemical properties of alkali-treated new cellulosic fiber from cotton shell," *International Journal of Polymer Analysis and Characterization* 21(4), 359-364. DOI: 10.1080/1023666X.2016.1160509

Rashid, B., Leman, Z., Jawaid, M., Ghazali, M. J., and Ishak, M. R. (2016). "Physicochemical and thermal properties of lignocellulosic fiber from sugar palm fibers: Effect of treatment," *Cellulose* 23(5), 1-12. DOI: 10.1007/s10570-016-1005-z

Ray, D., and Sarkar, B. K. (2001). "Characterization of alkali-treated jute fibers for physical and mechanical properties," *Journal of Applied Polymer Science* 80(7), 1013-1020. DOI: 10.1002/app.1184

Razali, N., Salit, M. S., Jawaid, M., Ishak, M. R., and Lazim, Y. (2015). "A study on chemical composition, physical, tensile, morphological, and thermal properties of roselle fibre: Effect of fibre maturity," *BioResources* 10(1), 1803-1823.

Reddy, N., and Yang, Y. (2015). "Biocomposites using lignocellulosic agricultural residues as reinforcement," in: *Innovative Biofibers from Renewable Resources*, Springer, Berlin Heidelberg, pp. 391-417. DOI: 10.1007/978-3-662-45136-6_68

Rong, M. Z., Zhang, M. Q., Liu, Y., Yang, G. C., and Zeng, H. M. (2001). "The effect of fiber treatment on the mechanical properties of unidirectional sisal-reinforced epoxy composites," *Composites Science and Technology* 61(10), 1437-1447. DOI: 10.1016/S0266-3538(01)00046-X

Sahari, J., Sapuan, S. M., Ismarrubie, Z. N., and Rahman, M. (2012). "Physical and chemical properties of different morphological parts of sugar palm fibres," *Fibres and Textiles in Eastern Europe* 91(2), 21-24.

Sanyang, M. L., Sapuan, S. M., Jawaid, M., Ishak, M. R., and Sahari, J. (2016a). "Effect of sugar palm-derived cellulose reinforcement on the mechanical and water barrier properties of sugar palm starch biocomposite films," *BioResources* 11(2), 4134-4145. DOI: 10.15376/biores.11.2.4134-4145

Sanyang, M. L., Sapuan, S. M., Jawaid, M., Ishak, M. R., and Sahari, J. (2016b). "Recent developments in sugar palm (*Arenga pinnata*) based biocomposites and their potential industrial applications: A review," *Renewable and Sustainable Energy Reviews* 54, 533-549. DOI: 10.1016/j.rser.2015.10.037

Segal, L., Creely, J. J., Martin, A. E., and Conrad, C. M. (1959). "An empirical method for estimating the degree of crystallinity of native cellulose using the X-ray diffractometer," *Textile Research Journal* 29(10), 786-794. DOI: 10.1177/004051755902901003

Sgriccia, N., Hawley, M. C., and Misra, M. (2008). "Characterization of natural fiber surfaces and natural fiber composites," *Composites Part A: Applied Science and Manufacturing* 39(10), 1632-1637. DOI: 10.1016/j.compositesa.2008.07.007

Shafizadeh, F., and Chin, P. P. S. (1977). "Thermal deterioration of wood," in: *Wood Technology: Chemical Aspects*, I. S. Goldstein (ed.), ACS Symposium Series 43, pp. 57-81. DOI: 10.1021/bk-1977-0043.ch005

Sheltami, R. M., Abdullah, I., Ahmad, I., Dufresne, A., and Kargarzadeh, H. (2012). "Extraction of cellulose nanocrystals from mengkuang leaves (*Pandanus tectorius*)," *Carbohydrate Polymers* 88(2), 772-779. DOI: 10.1016/j.carbpol.2012.01.062

Sonia, A., and Dasan, K. P. (2014). "Barrier properties of celluloses microfibers (CMF)/ethylene-co-vinyl acetate (EVA)/composites," *Composite Interfaces* 21(3), 233-250. DOI: 10.1080/15685543.2014.856644

Sun, R. C., and Tomkinson, J. (2002). "Comparative study of organic solvent-soluble and water-soluble lipophilic extractives from wheat straw. 2: Spectroscopic and thermal analysis," *Journal of Wood Science* 48(3), 222-226. https://doi.org/10.1007/BF00771371

Sun, X. F., Xu, F., Sun, R. C., Fowler, P., and Baird, M. S. (2005). "Characteristics of degraded cellulose obtained from steam-exploded wheat straw," *Carbohydrate Research* 340(1), 97-106. DOI: 10.1016/j.carres.2004.10.022

TAPPI (2006). "Acid-insoluble lignin in wood and pulp," TAPPI T 222, om-02. (1-14).

TAPPI (1999). "Alpha-, beta- and gamma-cellulose in pulp," TAPPI 203, cm-99. (1-5).

Talib, R. A., Tawakkal, I. S. M. A., and Khalina, A. (2011). "The influence of mercerised kenaf fibres reinforced polylactic acid composites on dynamic mechanical analysis," *Key Engineering Materials 471–472*, 815-820. DOI: 10.4028/www.scientific.net/KEM.471-472.815

Tan, I. S., and Lee, K. T. (2014). "Enzymatic hydrolysis and fermentation of seaweed solid wastes for bioethanol production: An optimization study," *Energy* 78, 53-62. DOI: 10.1016/j.energy.2014.04.080

Tawakkal, I. S. M., Talib, R., Abdan, K., and Ling, C. N. (2012). "Mechanical and physical properties of kenaf- derived cellulose (KDC)-filled polylactic acid (PLA) composites," *BioResources 7*(2), 1643-1655. DOI: 10.15376/biores.7.2.1643-1655

Tee, Y. B., Talib, R., Abdan, K., Chin, N. L., Basha, R. K., and Md Yunos, K. F. (2013). "Thermally grafting aminosilane onto kenaf-derived cellulose and its influence on the thermal properties of poly(lactic acid) composites," *BioResources* 8(3), 4468-4483. DOI: 10.15376/biores.8.3.4468-4483

Ticoalu, A., Aravinthan, T., and Cardona, F. (2013). "A review on the characteristics of gomuti fibre and its composites with thermoset resins," *Journal of Reinforced Plastics and Composites* 32(2), 124-136. DOI: 10.1177/0731684412463109

Tomlinson, P. B. (1962). "The Leaf base in palms its morphology and mechanical biology," *Journal of the Arnold Arboretum* 43(1), 23-50.

Wang Yueping, Wang Ge, Cheng Haitao, Tian Genlin, Liu Zheng, Xiao Qun Feng, Zhou Xiangqi, Han Xiaojun, and Gao Xushan. (2010). "Structures of Bamboo fiber for textiles," *Textile Research Journal* 80(4), 334-343. DOI: 10.1177/0040517509337633

Wise, L. E., Murphy, M., and D'Addieco, A. A. (1946). "Chlorite, holocellulose, its fractionation and bearing on summative wood analysis and on studies on the hemicellulose," *Paper Trade Journal* 122(2), 35-43.

Xiao, B., Sun, X., and Sun, R. (2001). "Chemical, structural, and thermal characterizations of alkali-soluble lignins and hemicelluloses, and cellulose from maize stems, rye straw, and rice straw," *Polymer Degradation and Stability* 74(2), 307-319. DOI: 10.1016/S0141-3910(01)00163-X

Yang, H., Yan, R., Chen, H., Lee, D. H., and Zheng, C. (2007). "Characteristics of hemicellulose, cellulose and lignin pyrolysis," *Fuel* 86(12–13), 1781-1788. DOI: 10.1016/j.fuel.2006.12.013

Yasim-Anuar, T. A. T., Ariffin, H., Norrrahim, M. N. F., and Hassan, M. A. (2017). "Factors affecting spinnability of oil palm mesocarp fiber cellulose solution for the production of microfiber," *BioResources* 12(1), 715-734. DOI: 10.15376/biores.12.1.715-734

Article submitted: July 9, 2017; Peer review completed: August 26, 2017; Revised version received: September 19, 2017; Accepted: September 27, 2017; Published: October 4, 2017.
DOI: 10.15376/biores.12.4.8734-8754